SANDIA REPORT
SAND2020-4428
Printed April 2020

Sandia National Laboratories

Two-Channel Monopulse Antenna Null Steering

Armin W Doerry, Douglas L Bickel

Prepared by
Sandia National Laboratories
Albuquerque, New Mexico
87185 and Livermore,
California 94550

Issued by Sandia National Laboratories, operated for the United States Department of Energy by National Technology & Engineering Solutions of Sandia, LLC.

Available to DOE and DOE contractors from
U.S. Department of Energy
Office of Scientific and Technical Information
P.O. Box 62
Oak Ridge, TN 37831

Telephone: (865) 576-8401
Facsimile: (865) 576-5728
E-Mail: reports@osti.gov
Online ordering: http://www.osti.gov/scitech

Available to the public from
U.S. Department of Commerce
National Technical Information Service
5301 Shawnee Rd
Alexandria, VA 22312

Telephone: (800) 553-6847
Facsimile: (703) 605-6900
E-Mail: orders@ntis.gov
Online order: https://classic.ntis.gov/help/order-methods/

Abstract

Traditional dual-channel phase-monopulse and amplitude-monopulse antenna systems might electrically steer their difference-channel nulls by suitably adjusting characteristics of their constituent beams or lobes. A phase-monopulse systems' null might be steered by applying suitable relative phase shifts. An amplitude-monopulse systems' null might be steered by applying a suitable relative beam amplitude scaling. The steering of the null might be employed by a continuously mechanically-scanning antenna to stabilize the null direction over a series of radar pulses.

Acknowledgements

This report was funded by General Atomics Aeronautical Systems, Inc. (GA-ASI) Mission Systems under Cooperative Research and Development Agreement (CRADA) SC08/01749 between Sandia National Laboratories and GA-ASI.

General Atomics Aeronautical Systems, Inc. (GA-ASI), an affiliate of privately-held General Atomics, is a leading manufacturer of Remotely Piloted Aircraft (RPA) systems, radars, and electro-optic and related mission systems, including the Predator®/Gray Eagle®-series and Lynx® Multi-mode Radar.

Contents

List of Figures

Acronyms and Definitions

1-D, 2-D, 3-D	1-, 2-, 3-Dimesional
AM	Amplitude Monopulse
CNR	Clutter to Noise Ratio
DMTI	Dismount Moving Target Indicator
DOA	Direction of Arrival
DPCA	Displaced Phase Center Antenna
GMTI	Ground Moving Target Indicator
MTI	Moving Target Indicator
MVDR	Minimum Variance Distortionless Response
PM	Phase Monopulse
RX	Receive or Receiver
TX	Transmit or Transmitter

Foreword

This report details the results of an academic study. It does not presently exemplify any modes, methodologies, or techniques employed by any operational system known to the authors.

Classification

The specific mathematics and algorithms presented herein do not bear any release restrictions or distribution limitations.

This report formalizes preexisting informal notes and other documentation on the subject matter herein.

Author Contact Information

Armin Doerry	awdoerr@sandia.gov	505-845-8165
Doug Bickel	dlbicke@sandia.gov	505-845-9038

1 Introduction and Background

IEEE Standard 145-1983 defines Monopulse as "Simultaneous lobing whereby direction-finding information is obtainable from a single pulse."[1] We note that there is no mention of the number of beams, phase-centers, or lobes, nor any indication of an antenna topology to achieve such single-pulse direction finding. Nevertheless, colloquially the term "monopulse" is often construed to mean merely two lobes offset from each other in some direction. Furthermore, we stipulate two principal monopulse configurations;

1. Phase Monopulse (PM), whereby typically the antenna pattern individual lobes have distinct phase-centers, but individual lobes have a common (i.e. parallel) boresight direction, and

2. Amplitude Monopulse (AM), whereby typically the antenna pattern individual lobes have identical phase-centers, but individual lobes have distinct individual boresight directions.

We recognize that hybrid configurations do exist but are beyond the scope of this report.

Monopulse antennas are discussed in detail in a text by Sherman and Barton.[2]

Two principal applications of monopulse antennas are

1. Determining the Direction of Arrival (DOA) of a received signal, and

2. Mitigating problematic signal energy by nulling a particular DOA.

In both cases, this is achieved by differencing the two lobes (or some feature of the lobes), and often also includes a normalization operation whereby the difference is divided by the sum of the same two lobes, or a similar reference signal.

The null direction is typically coincident with the electrical boresight of the overall antenna. We differentiate this from mechanical boresight of the antenna, usually defined as the intended direction of peak gain for the overall antenna, typically entire aperture, or perhaps the transmit antenna. Usually it is desired that these boresights match, or at least that the differences are well-understood and well-characterized, usually meaning well-calibrated.

In this report we concern ourselves with nulling a particular DOA, and furthermore adjusting the nulled DOA by electrically manipulating the received signal data, after it has been collected and stored. We concern ourselves with just two lobes. We do so with two particular applications in mind, these being

1. Nulling a ground clutter return for an airborne weather mapping radar, and

2. Stabilizing the azimuthal null direction over a set of pulses for a continuously mechanically-scanning antenna.

Other applications can also be easily conjured.

We are mindful that often a two-channel monopulse configuration, instead of making available the received data from the individual lobes, will provide sum and difference combinations of the signals from those lobes. Circuits for generating sum and difference channels go by various names, including "monopulse network," "monopulse comparator," "hybrid," "magic-T network," and others. This has been a common practice from the early days of monopulse radars employed as tracking radars, and endures. However, doing so with hardware (or at all) is not an essential feature for DOA determination and manipulation.

Furthermore, these circuits often exhibit their own non-ideal behaviors, generating errors with respect to the desired behavior of the individual lobes. Such errors can be substantially reduced by appropriate calibration of the antenna. Doing so is beyond the scope of this report.

However, we do stipulate that the techniques discussed later in this report are tantamount to inducing precise "errors" to control the characteristics of the antenna beam lobes. Monopulse errors are discussed extensively in an earlier report by Bickel.[3] In addition, it has been known for some time that linear combinations of the sum and difference beams can be used to adjust clutter cancellation in applications such as in Displaced Phase Center Antenna (DPCA) systems.[4]

We offer the following references as additional background information.

Phase Monopulse

Sandia National Laboratories Report SAND2015-2310 discusses DOA measurements from multiple phase-centers.[5]

Sandia National Laboratories Report SAND2015-2311 discusses limits to clutter cancellation in multi-aperture GMTI data.[6]

Sandia National Laboratories Report SAND2015-9566 discusses phase-centers of subapertures in a tapered aperture array.[7]

Amplitude Monopulse

Sandia National Laboratories Report SAND2015-4113 discusses a single-axis three-beam amplitude-monopulse antenna, in addition to a dual-beam antenna.[8]

Sandia National Laboratories Report SAND2013-10635 discusses the location of the phase-center for a dish antenna.[9]

2 Phase Monopulse

Consider a phase-monopulse antenna, with lobes generated by two distinct offset phase centers, but otherwise identical characteristics. We model this antenna with a one-dimensional representation of a uniformly illuminated aperture given in Figure 1.

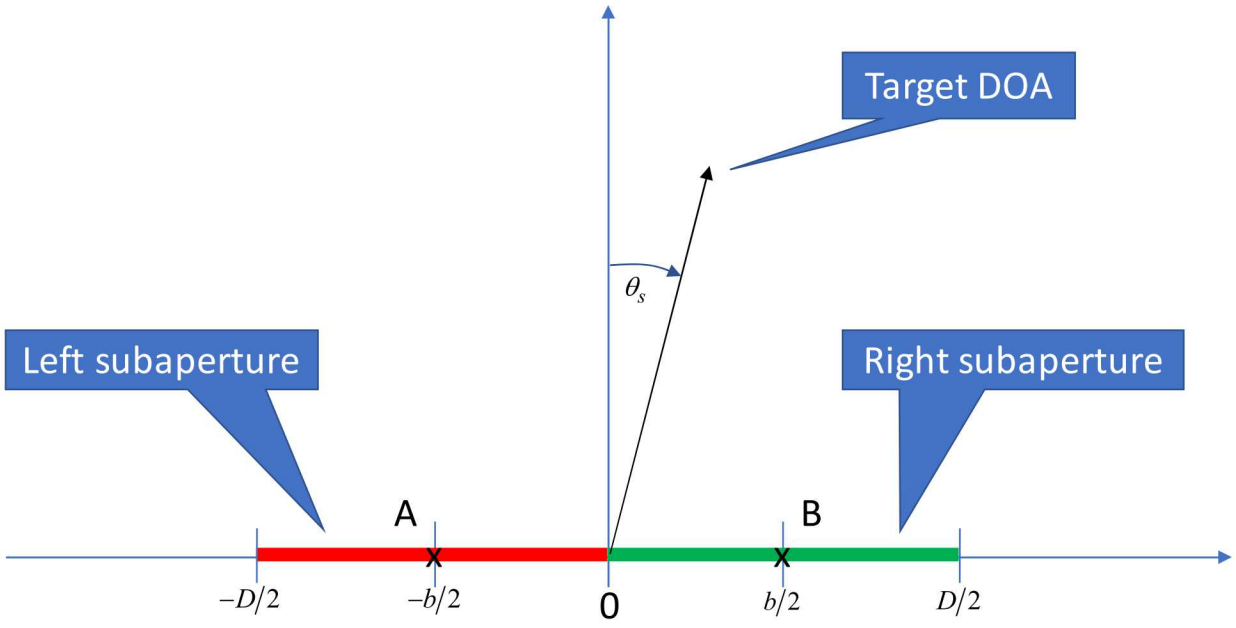

Figure 1. One-dimensional representation of a phase-monopulse antenna.

The overall aperture will have nominal beamwidth

$$\theta_a = \frac{\lambda}{D}, \tag{1}$$

where

D = nominal length of the total aperture, and
λ = nominal wavelength of the radar signal. (2)

For a target at some distant range from the antenna, we identify the ranges to the two phase-centers as

$$r_{s,A} = r_s + \frac{b}{2}\sin\theta_s, \text{ and}$$
$$r_{s,B} = r_s - \frac{b}{2}\sin\theta_s, \tag{3}$$

where

r_s = range from the origin to the target,

b = baseline separation of the individual phase centers, and

θ_s = DOA of the target from the reference boresight direction of the antenna. (4)

Presuming a monostatic radar, with transmit signal emanating from the origin, a radar echo return signal will exhibit phase that depends on total two-way range, allowing us to write the impact on the two phase-centers as being multiplied by the factors

$$X_A(\theta_s) = e^{-j\frac{2\pi}{\lambda}\left(2r_s + \frac{b}{2}\sin\theta_s\right)}, \text{ and}$$
$$X_B(\theta_s) = e^{-j\frac{2\pi}{\lambda}\left(2r_s - \frac{b}{2}\sin\theta_s\right)}. \quad (5)$$

We are ignoring subaperture-beam amplitude effects, as they should be identical. The difference between signals received by phase-centers A and B will then be proportional to the factor

$$\Delta_{A,B}(\theta_s) = X_A(\theta_s) - X_B(\theta_s), \quad (6)$$

which can be expanded and simplified to

$$\Delta_{A,B}(\theta_s) = -2je^{-j\frac{4\pi}{\lambda}r_s}\sin\left(\frac{\pi b}{\lambda}\sin\theta_s\right). \quad (7)$$

For reference, the sum of the signals received by phase-centers A and B will then be proportional to the factor

$$\Sigma_{A,B}(\theta_s) = X_A(\theta_s) + X_B(\theta_s), \quad (8)$$

which can be expanded and simplified to

$$\Sigma_{A,B}(\theta_s) = 2e^{-j\frac{4\pi}{\lambda}r_s}\cos\left(\frac{\pi b}{\lambda}\sin\theta_s\right). \quad (9)$$

Typically, to extract an angel measure, the ratio of difference to sum signals is calculated, which yields

$$\frac{\Delta_{A,B}(\theta_s)}{\Sigma_{A,B}(\theta_s)} = j\tan\left(-\frac{\pi b}{\lambda}\sin\theta_s\right). \quad (10)$$

Note that this ratio is purely imaginary (in the complex sense). The argument of the tangent function defines an error signal that is proportional to the target DOA, and nearly linear for small DOA offsets. This may be rewritten as

$$-\frac{\pi b}{\lambda}\sin\theta_s = k_m\left(\frac{\theta_s}{\theta_a}\right). \tag{11}$$

where the slope of this relationship with respect to θ_s at $\theta_s = 0$ may be written as

$$k_m = \theta_a \frac{d}{d\theta_s}\left(-\frac{\pi b}{\lambda}\sin\theta_s\right)\Bigg|_{\theta_s=0} = -\pi\frac{b}{D}. \tag{12}$$

For a baseline that is half the antenna dimension, this becomes $k_m = -\pi/2$. Furthermore, we observe that Eq. (7) indicates a null response at $\theta_s = 0$. These define typical ideal monopulse behavior.

Summarizing, for small DOA offsets, using small angle approximations, we may estimate the target DOA as

$$\hat{\theta}_s = \frac{\theta_a}{k_m}\left(-j\frac{\Delta_{A,B}(\theta_s)}{\Sigma_{A,B}(\theta_s)}\right). \tag{13}$$

Note that the multiplication by $-j$ in this case is tantamount to merely taking the imaginary part of the ratio, that is

$$\hat{\theta}_s = \frac{\theta_a}{k_m}\mathrm{Im}\left(\frac{\Delta_{A,B}(\theta_s)}{\Sigma_{A,B}(\theta_s)}\right). \tag{14}$$

2.1 Adjusting the Null Direction

With malice aforethought we now add a relative phase shift between phase centers such that

$$X_A(\theta_s) = e^{-j\frac{2\pi}{\lambda}\left(2r_s+\frac{b}{2}\sin\theta_s\right)}e^{j\frac{\phi}{2}}, \text{ and}$$
$$X_B(\theta_s) = e^{-j\frac{2\pi}{\lambda}\left(2r_s-\frac{b}{2}\sin\theta_s\right)}e^{-j\frac{\phi}{2}}, \tag{15}$$

where the phase shift term

$$\phi = \text{relative phase shift added between phase-centers.} \tag{16}$$

Sum and difference signals now become

$$\Sigma_{A,B}(\theta_s) = 2e^{-j\frac{4\pi}{\lambda}r_s}\cos\left(\frac{\pi b}{\lambda}\sin\theta_s - \frac{\phi}{2}\right), \text{ and}$$

$$\Delta_{A,B}(\theta_s) = -2je^{-j\frac{4\pi}{\lambda}r_s}\sin\left(\frac{2\pi b}{\lambda}\sin\theta_s - \frac{\phi}{2}\right). \tag{17}$$

We now set this phase shift to correspond to a particular DOA, namely we let

$$\phi = \frac{4\pi b}{\lambda}\sin\theta_n, \tag{18}$$

where we define a new angle

$$\theta_n = \text{DOA of resulting null.} \tag{19}$$

We illustrate this in Figure 2.

Note that if the relative phase-shift ϕ is undesired, then it is often termed a "pre-comparator" error, which typically requires mitigation via calibration.

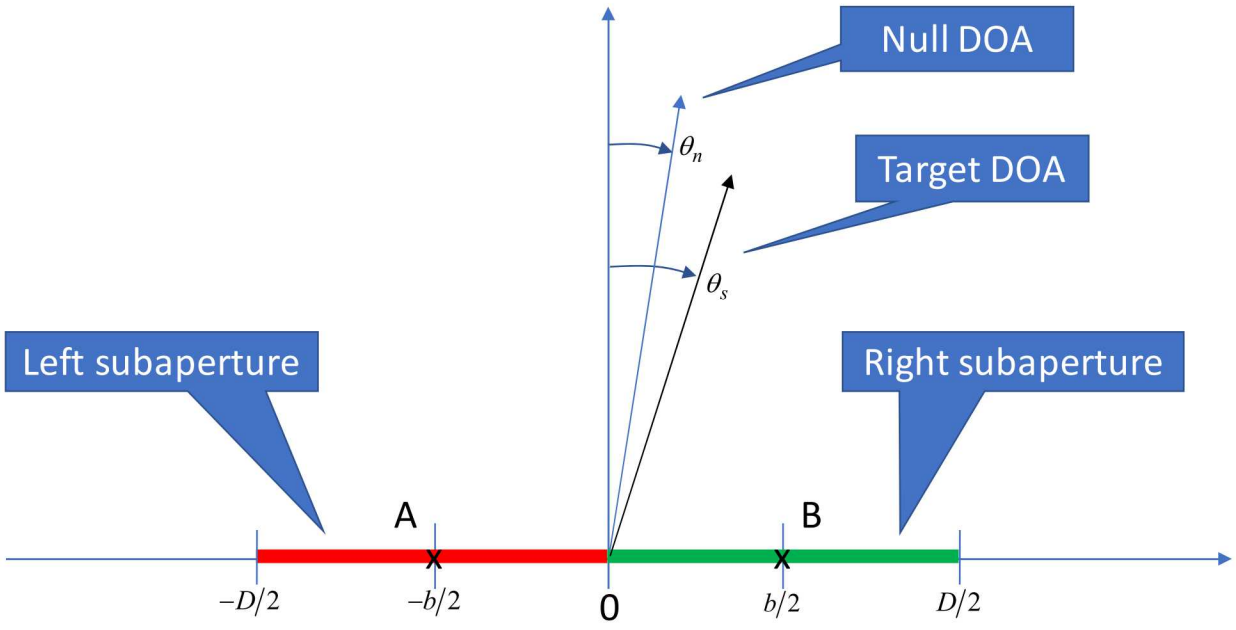

Figure 2. Angle definition for a selected null DOA.

This allows us to write

$$\Sigma_{A,B}(\theta_s) = 2e^{-j\frac{4\pi}{\lambda}r_s}\cos\left(\frac{2\pi b}{\lambda}(\sin\theta_s - \sin\theta_n)\right), \text{ and}$$

$$\Delta_{A,B}(\theta_s) = -2je^{-j\frac{4\pi}{\lambda}r_s}\sin\left(\frac{\pi b}{\lambda}(\sin\theta_s - \sin\theta_n)\right). \tag{20}$$

Clearly, the sum channel exhibits a peak, and the difference channel exhibits a null, both which are shifted to $\theta_s = \theta_n$. For small angles about the null direction, we may use a Taylor series expansion with small angle approximations to calculate the monopulse slope as

$$k_m = -\pi\frac{b\cos\theta_n}{D}. \tag{21}$$

We observe that there is very similar to Eq. (12), except for a very slight shortening of the effective baseline due to its projection in the direction of θ_n.

For small DOA offsets, using small angle approximations, we may now estimate the target DOA as

$$\hat{\theta}_s = \theta_n + \frac{\theta_a}{k_m}\left(-j\frac{\Delta_{A,B}(\theta_s)}{\Sigma_{A,B}(\theta_s)}\right). \tag{22}$$

We offer some comments.

- Typically, for antennas used in microwave radar systems, $D \gg \lambda$, such that the reference beamwidth $\theta_a \ll 1$, perhaps only a few single-digit degrees.

- Once radar data is received, digitized, and recorded, it is stuck with the transmit antenna beam characteristics that were used. In addition, it is stuck with the individual lobe characteristics of the collection; the nature of the subaperture characteristics during the collection.

- However, the combination of subaperture data, i.e. the different phase-centers' data, can be adjusted at will after the fact, subject only to the limitations of the transmit and receive-lobe beams.

- Nevertheless, the relatively narrow transmit beam implies no need for any large shift in difference-channel null angle.

For all these reasons, small-angle approximations are justified.

2.2 Stabilizing the Null Direction During a Scan

We now examine stabilizing a null DOA during a continuous scan. We will presume that the antenna is rotating about its center. Rotation about an offset point will add some complication, but is readily calculable. For simplicity, we will assume rotation about the center as is illustrated in Figure 3.

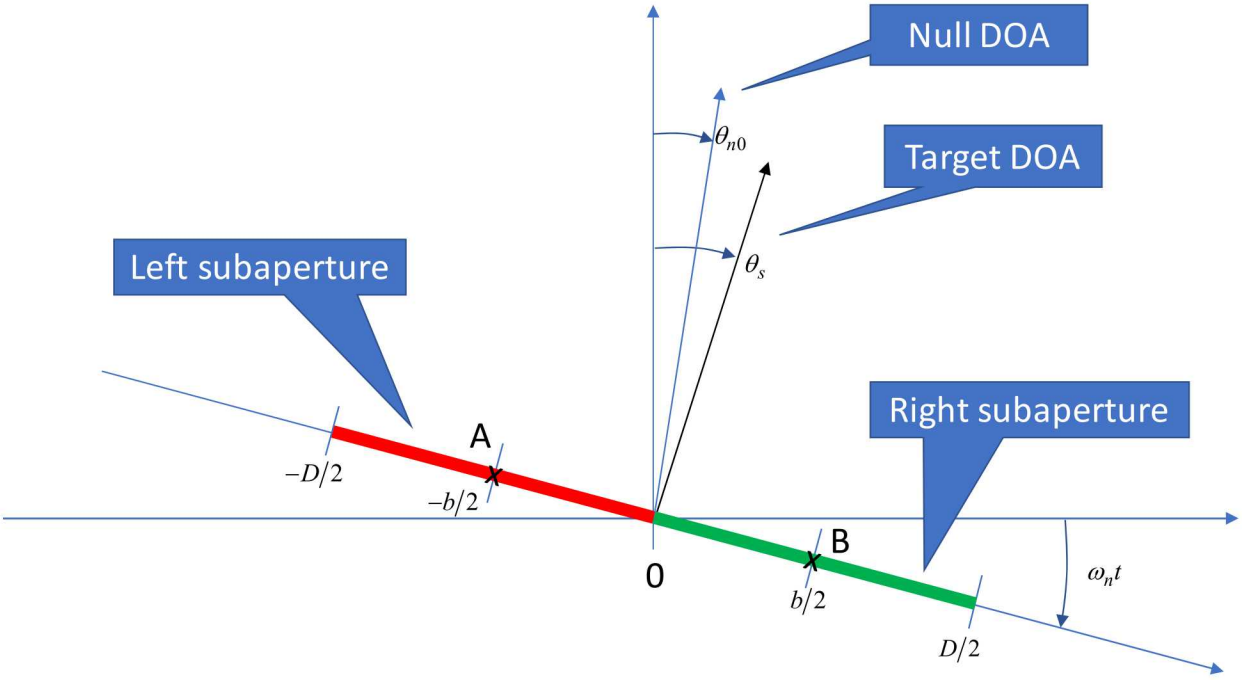

Figure 3. Angle definition for a continuously rotating phase-monopulse antenna.

The phase-centers will see time-varying signals of the form

$$X_A(\theta_s) = e^{-j\frac{2\pi}{\lambda}\left(2r_s + \frac{b}{2}\sin(\theta_s - \omega_n t)\right)} e^{j\frac{\phi(t)}{2}}, \text{ and}$$
$$X_B(\theta_s) = e^{-j\frac{2\pi}{\lambda}\left(2r_s - \frac{b}{2}\sin(\theta_s - \omega_n t)\right)} e^{-j\frac{\phi(t)}{2}}. \quad (23)$$

where

t = time relative to the center of the scan interval, with $-T/2 \le t \le T/2$,
T = the time interval over which we wish to stabilize the null direction,
ω_n = the angular velocity of the continuous scan, and
θ_s = the target DOA relative to the reference boresight direction at scan center. (24)

We now select a similarly time-varying phase adjustment given by

$$\phi(t) = \frac{2\pi b}{\lambda}\sin(\theta_{n0} - \omega_n t), \tag{25}$$

where

θ_{n0} = the stabilized null DOA, relative to the reference boresight direction at scan center. (26)

The relevant sum and difference channels become

$$\Sigma_{A,B}(\theta_s) = 2e^{-j\frac{4\pi}{\lambda}r_s}\cos\left(\frac{\pi b}{\lambda}\left(\sin(\theta_s - \omega_n t) - \sin(\theta_{n0} - \omega_n t)\right)\right), \text{ and}$$

$$\Delta_{A,B}(\theta_s) = -2je^{-j\frac{4\pi}{\lambda}r_s}\sin\left(\frac{\pi b}{\lambda}\left(\sin(\theta_s - \omega_n t) - \sin(\theta_{n0} - \omega_n t)\right)\right). \tag{27}$$

The sum channel still exhibits a peak at $\theta_s = \theta_{n0}$. The difference channel also still exhibits a null, still shifted to $\theta_s = \theta_{n0}$. For small angles about the null direction, we may use a Taylor series expansion with small angle approximations to calculate the monopulse slope as

$$k_m = -\pi\frac{b\cos(\theta_{n0} - \omega_n t)}{D}. \tag{28}$$

Since we expect the time-varying angle $(\theta_{n0} - \omega_n t)$ to be small, the time-dependence of the monopulse slope is also very small. This suggests that we may continue to reasonably approximate

$$k_m \approx -\pi\frac{b}{D}. \tag{29}$$

We offer the comments,

- This entails that the phase-shifts applied to the respective phase-centers be time-dependent, as given in Eq. (25).
- For small angles typical of microwave monopulse operation, the monopulse slope will be slightly modulated with time, but likely negligibly.

“I had the right to remain silent... but I didn't have the ability.”
-- Ron White

3 Amplitude Monopulse

Consider an amplitude-monopulse antenna, with lobes generated at a common phase center, but with different lobe directions, and otherwise identical characteristics. We model this antenna with a one-dimensional representation of a uniformly illuminated aperture given in Figure 4.

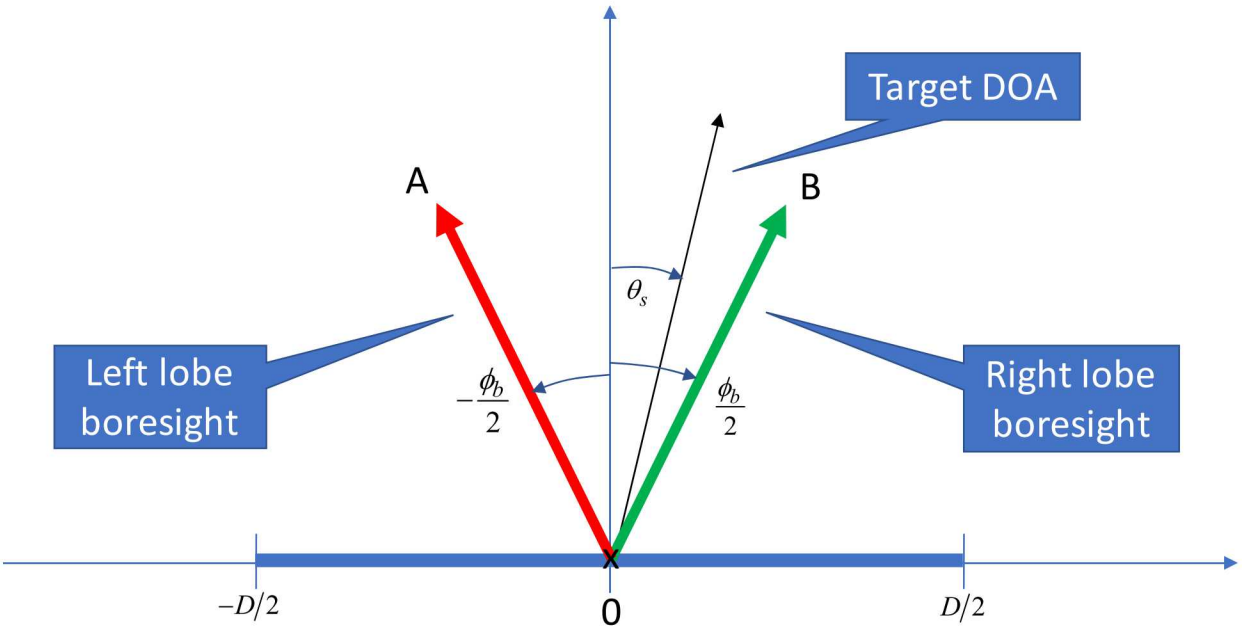

Figure 4. One-dimensional representation of an amplitude-monopulse antenna.

For a uniformly illuminated aperture, without any applied phase-ramp or other steering, the far-field antenna pattern is given by

$$G(\theta) = \int_{-D/2}^{D/2} e^{j\frac{2\pi}{\lambda} l \sin\theta} dl = D \frac{\sin\left(\pi \frac{D}{\lambda} \sin\theta\right)}{\pi \frac{D}{\lambda} \sin\theta} = D \,\mathrm{sinc}\left(\frac{1}{\theta_a} \sin\theta\right). \tag{30}$$

where

$$\mathrm{sinc}(z) = \frac{\sin(\pi z)}{\pi z}, \text{ and}$$
$$\theta_a = \lambda / D \,. \tag{31}$$

By applying linear phase-ramps across the aperture, we may squint the beams such that

$$G_A(\theta_s) = D\,\mathrm{sinc}\left(\frac{1}{\theta_a}\left(\cos\left(\frac{\phi_b}{2}\right)\sin\left(\theta_s+\frac{\phi_b}{2}\right)-\left(\cos\left(\theta_s+\frac{\phi_b}{2}\right)-1\right)\sin\left(\frac{\phi_b}{2}\right)\right)\right), \text{ and}$$

$$G_B(\theta_s) = D\,\mathrm{sinc}\left(\frac{1}{\theta_a}\left(\cos\left(\frac{\phi_b}{2}\right)\sin\left(\theta_s-\frac{\phi_b}{2}\right)+\left(\cos\left(\theta_s-\frac{\phi_b}{2}\right)-1\right)\sin\left(\frac{\phi_b}{2}\right)\right)\right), \tag{32}$$

where the squint angles are positive and negative halves of

ϕ_b = the angular separation of the two squinted lobes. (33)

The value for ϕ_b is generally desired to be such as to minimize the variance in any DOA angle measurement. This will depend on individual lobes' beam shapes.[2,8] For our uniformly illuminated aperture, the minimum DOA variance is in fact achieved with $\phi_b = 0.83\,\theta_a$.

In the neighborhoods of the lobes' peak responses we easily show that

$$\cos\left(\theta_s \pm \frac{\phi_b}{2}\right) \approx 1. \tag{34}$$

This allows us to reasonably approximate

$$G_A(\theta_s) = D\,\mathrm{sinc}\left(\frac{1}{\theta_a}\cos\frac{\phi_b}{2}\sin\left(\theta_s+\frac{\phi_b}{2}\right)\right), \text{ and}$$

$$G_B(\theta_s) = D\,\mathrm{sinc}\left(\frac{1}{\theta_a}\cos\frac{\phi_b}{2}\sin\left(\theta_s-\frac{\phi_b}{2}\right)\right). \tag{35}$$

Note that the lobes' widths increase with increasing squint-angles.

We offer the following additional comments.

- The squint angles for amplitude-monopulse antennas are generally a fraction of the beamwidth, that is

  $\phi_b < \theta_a$, where $\theta_a = \lambda/D$. (36)

- At microwave frequencies, these angles are fairly small, typically low-single-digit degrees. Consequently, we may assume in subsequent analysis that

  $$\cos\frac{\phi_b}{2} \approx 1. \tag{37}$$

- Furthermore, our interest is limited to the angular span between the lobes, or

  $$\frac{\phi_b}{2} \le \theta_s \le \frac{\phi_b}{2}. \tag{38}$$

For the expected lobes' small squint-angles we may reasonably simplify the lobe responses to

$$G_A(\theta_s) = D\,\mathrm{sinc}\left(\frac{1}{\theta_a}\sin\left(\theta_s + \frac{\phi_b}{2}\right)\right), \text{ and}$$
$$G_B(\theta_s) = D\,\mathrm{sinc}\left(\frac{1}{\theta_a}\sin\left(\theta_s - \frac{\phi_b}{2}\right)\right), \tag{39}$$

and perhaps further to

$$G_A(\theta_s) = D\,\mathrm{sinc}\left(\frac{1}{\theta_a}\left(\theta_s + \frac{\phi_b}{2}\right)\right), \text{ and}$$
$$G_B(\theta_s) = D\,\mathrm{sinc}\left(\frac{1}{\theta_a}\left(\theta_s - \frac{\phi_b}{2}\right)\right). \tag{40}$$

Sum and difference signals are now identified to be

$$\Sigma(\theta_s) = G_A(\theta_s) + G_B(\theta_s), \text{ and}$$
$$\Delta(\theta_s) = G_A(\theta_s) - G_B(\theta_s). \tag{41}$$

The ratio of difference to sum signals is calculated, and then expanded and linearized about the angle $\theta_s = 0$ to yield

$$\frac{\Delta(\theta_s)}{\Sigma(\theta_s)} \approx \left(\pi\cot\left(\pi\phi_b/2\theta_a\right) - \frac{1}{\phi_b/2\theta_a}\right)\frac{\theta_s}{\theta_a}. \tag{42}$$

From this we see a null at $\theta_s = 0$, and a monopulse slope given by

$$k_m = \theta_a \frac{d}{d\theta_s}\left(\frac{\Delta(\theta_s)}{\Sigma(\theta_s)}\right)\bigg|_{\theta_s=0} = \left(\pi\cot\left(\pi\phi_b/2\theta_a\right) - \frac{1}{\phi_b/2\theta_a}\right). \tag{43}$$

Recall that this is for small angles. For a an optimal $\phi_b \approx 0.83\,\theta_a$, this is on the order of $-\pi/2$.

Summarizing, for small DOA offsets, using small angle approximations, we may estimate the target DOA as

$$\hat{\theta}_s = \frac{\theta_a}{k_m}\mathrm{Re}\left(\frac{\Delta_{A,B}(\theta_s)}{\Sigma_{A,B}(\theta_s)}\right). \tag{44}$$

3.1 Adjusting the Null Direction

With malice aforethought we now add a relative amplitude adjustment to the lobes for the difference channel such that we create a new difference signal of the form

$$\Delta'(\theta_s) = (1+\beta) G_A(\theta_s) - (1-\beta) G_B(\theta_s), \tag{45}$$

where

$$\beta \text{ = amplitude adjustment factor.} \tag{46}$$

We note that in this formulation, and retaining the definitions in Eq. (41), we may also write

$$\Delta'(\theta_s) = \Delta(\theta_s) + \beta\, \Sigma(\theta_s). \tag{47}$$

We also note that the ratio of the new difference signal to the sum signal becomes

$$\frac{\Delta'(\theta_s)}{\Sigma(\theta_s)} = \frac{\Delta(\theta_s) + \beta\Sigma(\theta_s)}{\Sigma(\theta_s)} = \frac{\Delta(\theta_s)}{\Sigma(\theta_s)} + \beta. \tag{48}$$

We relate β to a specific angle θ_n by

$$\beta = \frac{\operatorname{sinc}\left(\frac{1}{\theta_a}\left(\theta_n - \frac{\phi_b}{2}\right)\right) - \operatorname{sinc}\left(\frac{1}{\theta_a}\left(\theta_n + \frac{\phi_b}{2}\right)\right)}{\operatorname{sinc}\left(\frac{1}{\theta_a}\left(\theta_n - \frac{\phi_b}{2}\right)\right) + \operatorname{sinc}\left(\frac{1}{\theta_a}\left(\theta_n + \frac{\phi_b}{2}\right)\right)}. \tag{49}$$

This is plotted in Figure 6. At this specific angle, with β so defined, we calculate

$$\Delta'(\theta_n) = 0, \tag{50}$$

thereby establishing θ_n as the new null direction. Recall that we generally choose to limit

$$|\theta_n| \le |\phi_b/2|. \tag{51}$$

Figure 5 illustrates scaling the amplitude monopulse lobes, and Figure 6 relates this scaling to a new null direction.

Figure 7 illustrates the monopulse ratio of Eq. (48) for the selected null direction $\theta_n/\theta_a = 0.25$. Note the null properly placed.

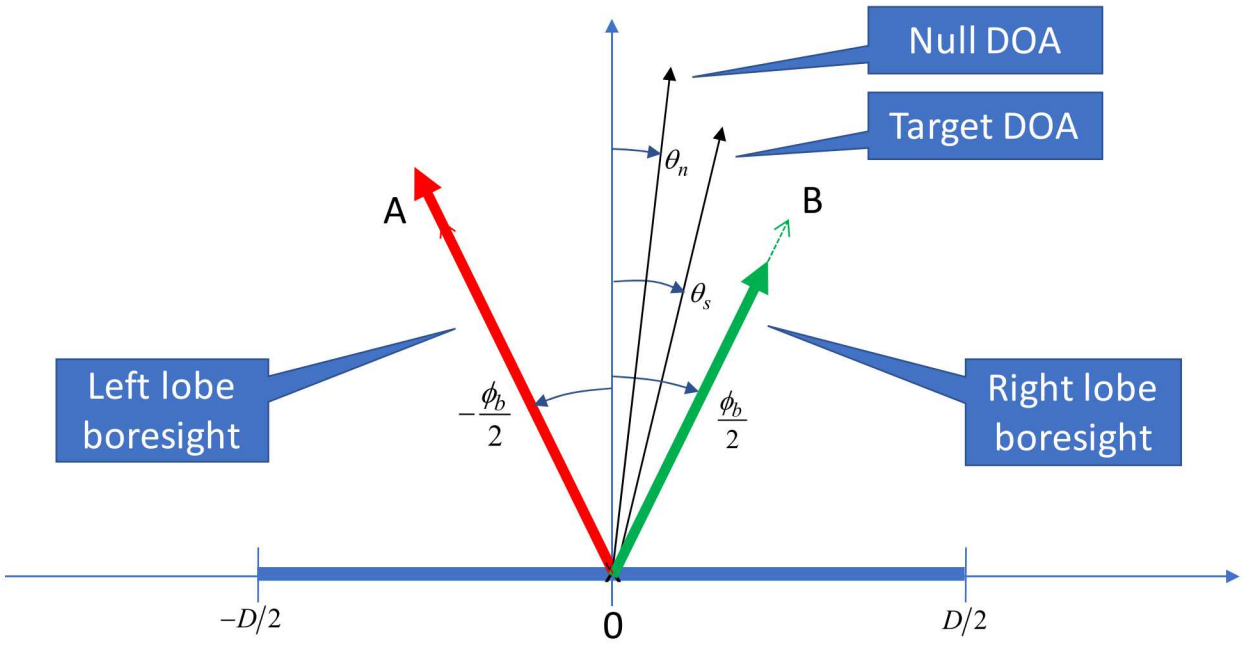

Figure 5. By scaling the amplitude monopulse lobes, the null is shifted to a new DOA.

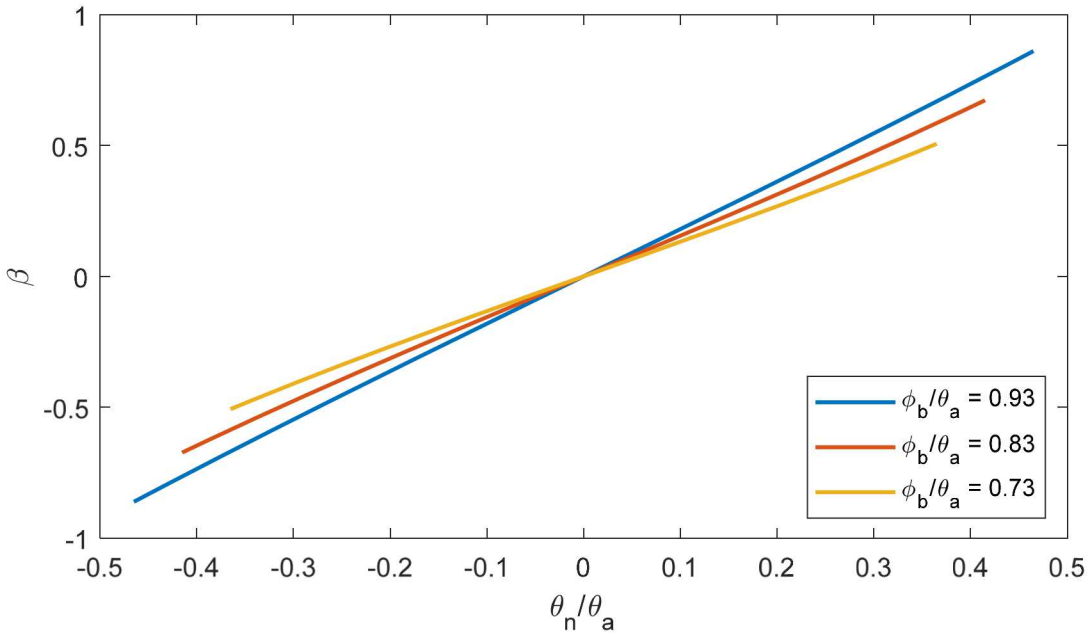

Figure 6. Relationship of β to null angle for various ϕ_b .

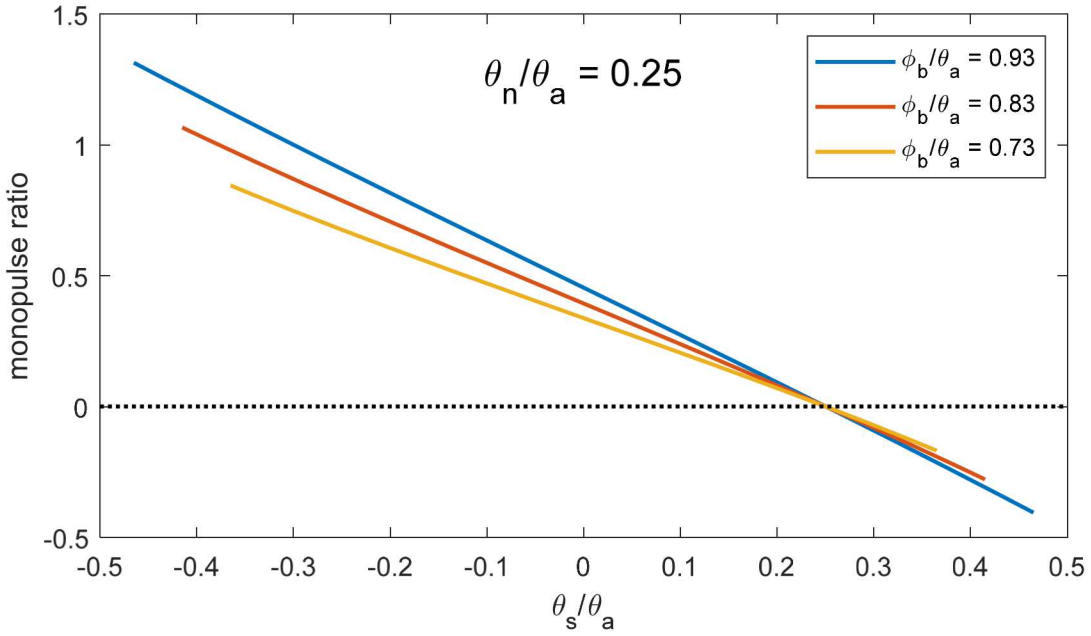

Figure 7. Example monopulse ratio for selected $\theta_n/\theta_a = 0.25$.

The monopulse slope in the region of this null is calculated as

$$k_m = \theta_a \frac{d}{d\theta_s}\left(\frac{\Delta'(\theta_s)}{\Sigma(\theta_s)}\right)\Bigg|_{\theta_s=\theta_n}$$

$$= \frac{2\left(\begin{array}{l}\left(\frac{\theta_n-\phi_b/2}{\theta_a}\right)^2\left(\begin{array}{l}\pi\left(\frac{\theta_n+\phi_b/2}{\theta_a}\right)\cos\left(\pi\left(\frac{\theta_n+\phi_b/2}{\theta_a}\right)\right)\\ -\sin\left(\pi\left(\frac{\theta_n+\phi_b/2}{\theta_a}\right)\right)\end{array}\right)\operatorname{sinc}\left(\frac{\theta_n-\phi_b/2}{\theta_a}\right)\\ -\left(\frac{\theta_n+\phi_b/2}{\theta_a}\right)^2\left(\begin{array}{l}\pi\left(\frac{\theta_n-\phi_b/2}{\theta_a}\right)\cos\left(\pi\left(\frac{\theta_n-\phi_b/2}{\theta_a}\right)\right)\\ -\sin\left(\pi\left(\frac{\theta_n-\phi_b/2}{\theta_a}\right)\right)\end{array}\right)\operatorname{sinc}\left(\frac{\theta_n+\phi_b/2}{\theta_a}\right)\end{array}\right)}{\pi\left(\frac{\theta_n^2-\phi_b^2/4}{\theta_a^2}\right)^2\left(\operatorname{sinc}\left(\frac{\theta_n-\phi_b/2}{\theta_a}\right)+\operatorname{sinc}\left(\frac{\theta_n+\phi_b/2}{\theta_a}\right)\right)^2}. \quad (52)$$

This slope of the monopulse ratio in the neighborhood of the null is plotted in Figure 8. Note that the monopulse slope is also reasonably stable over fractions of the reference beamwidth.

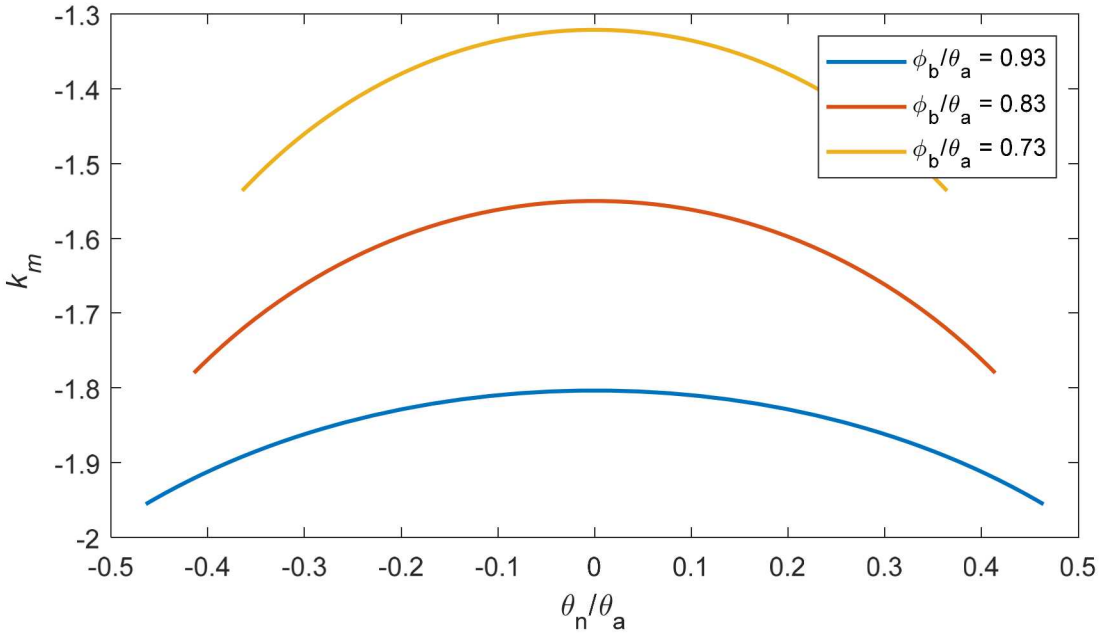

Figure 8. Monopulse slope in the neighborhood of the null as a function of relative null angle.

3.2 Stabilizing the Null Direction During a Scan

We now examine stabilizing a null DOA during a continuous scan. We will presume that the antenna is rotating about its center. Rotation about an offset point will add some complication, but is readily calculable. For simplicity, we will assume rotation about the center as is illustrated in Figure 9.

The lobes will see time-varying signals of the approximate form

$$G_A(\theta_s - \omega_n t) = D\,\mathrm{sinc}\left(\frac{1}{\theta_a}\left(\theta_s - \omega_n t + \frac{\phi_b}{2}\right)\right), \text{ and}$$
$$G_B(\theta_s - \omega_n t) = D\,\mathrm{sinc}\left(\frac{1}{\theta_a}\left(\theta_s - \omega_n t - \frac{\phi_b}{2}\right)\right). \tag{53}$$

We now create sum and difference signals of the form

$$\Sigma(\theta_s - \omega_n t) = G_A(\theta_s - \omega_n t) + G_B(\theta_s - \omega_n t),$$
$$\Delta(\theta_s - \omega_n t) = G_A(\theta_s - \omega_n t) - G_B(\theta_s - \omega_n t), \text{ and}$$
$$\Delta'(\theta_s - \omega_n t) = \Delta(\theta_s - \omega_n t) + \beta(t)\,\Sigma(\theta_s - \omega_n t), \tag{54}$$

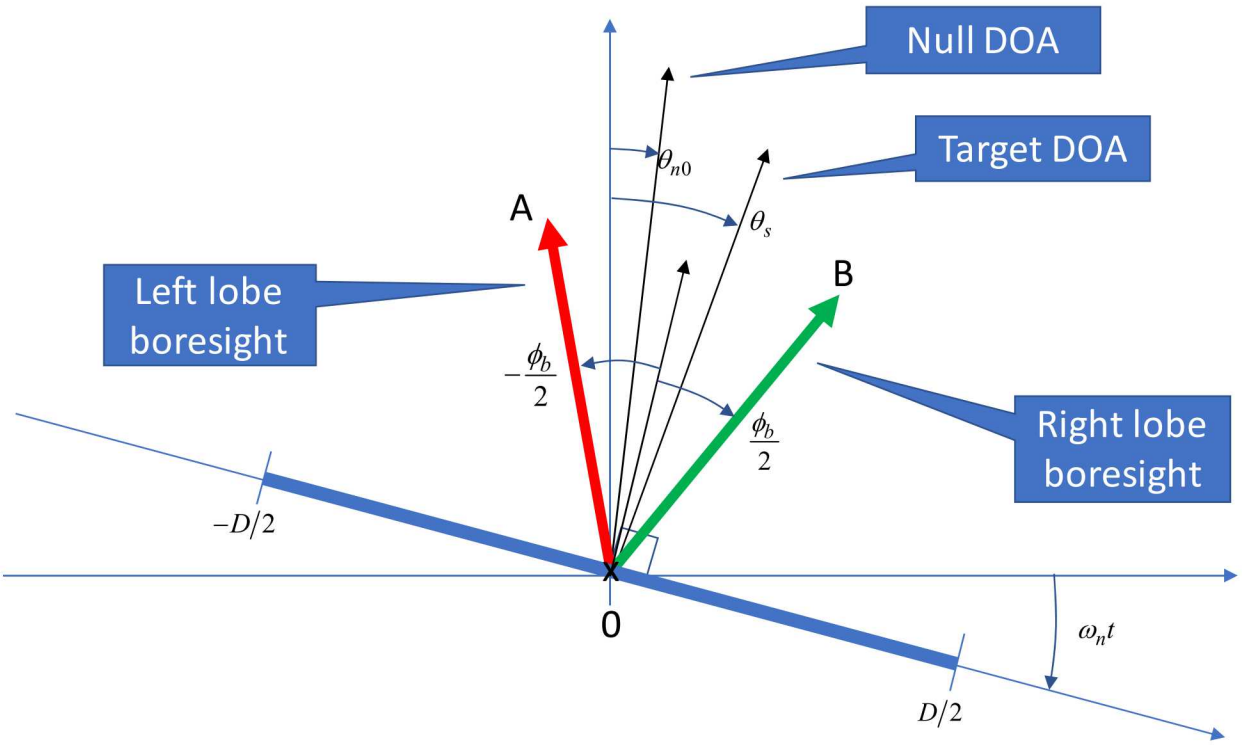

Figure 9. Angle definition for a continuously rotating amplitude-monopulse antenna.

where the varying scaling parameter is calculated as

$$\beta(t)=\frac{\operatorname{sinc}\left(\frac{1}{\theta_a}\left(\theta_{n0}-\omega_n t-\frac{\phi_b}{2}\right)\right)-\operatorname{sinc}\left(\frac{1}{\theta_a}\left(\theta_{n0}-\omega_n t+\frac{\phi_b}{2}\right)\right)}{\operatorname{sinc}\left(\frac{1}{\theta_a}\left(\theta_{n0}-\omega_n t-\frac{\phi_b}{2}\right)\right)+\operatorname{sinc}\left(\frac{1}{\theta_a}\left(\theta_{n0}-\omega_n t+\frac{\phi_b}{2}\right)\right)}. \tag{55}$$

With $\beta(t)$ so defined, we calculate

$$\Delta'\left(\theta_{n0}-\omega_n t\right)=0\,, \tag{56}$$

thereby establishing θ_{n0} as the new stabilized null direction. This means that any target with a DOA equal to θ_{n0} will see a null response, regardless of the antenna orientation, i.e. the specific time *t*.

The monopulse slope now becomes the expression in Eq. (52) except with the null direction now becoming time varying, namely where $\theta_n \to \left(\theta_{n0}-\omega_n t\right)$. This of course means the monopulse slope itself becomes time-varying, fluctuating as Figure 9 might suggest.

4 Additional Comments

In this section we look at a couple of other methods regarding null steering that can be accomplished in signal processing. The first is an angle blanking, and the second is a cancellation. In all of this we recall that the underlying purpose for the null steering is to remove energy reflecting from an unwanted direction in order to improve detection in the intended direction.

4.1 Angle blanking

A very simplified concept is to estimate the angles from the monopulse to the target area and "blank" those target echoes that exhibit angles that are undesirable. This is a "brute force" method that generates large nulls at the cost of discarding information. An issue with this blanking is that it removes all energy in the blanked resolution cell, some of which may be from the intended direction.

4.2 Cancellation

Another method would be to use the monopulse information in a manner similar to clutter cancellation. In cancellation, we use some a priori information to "steer" nulls on a pixel basis. For example, we may use a digital elevation model to map range pixels to an elevation, or we may use Doppler frequency to map angles for stationary clutter. We can then form a cancellation "beam" at a given pixel as a weighting of the monopulse signal as

$$x(k) = \mathbf{w}^H(\theta_k)\begin{bmatrix}\Sigma(k)\\ \Delta(k)\end{bmatrix}, \tag{57}$$

where we are considering the k^{th} pixel, and $\mathbf{w}$ is a weighting vector assuming some choice of the angle, θ_k, for the k^{th} pixel based upon the a priori information used. $\Sigma(k)$ and $\Delta(k)$ are the sum and difference values observed for the k^{th} pixel, respectively. The superscript "*H*" implies the Hermitian transpose of the weight vector, whereas later a superscript "*T*" is the simple transpose. There are multiple ways to choose the weight vector, and we will discuss two possibilities.

The first way would be to choose the weights to minimize the return for a given pixel from a specific direction, in other words, aim the null at a specific target angle. By inspection, if we wish to minimize $x(k)$ for the pixel in a given direction, θ_k, then we set the weighting to a scaled version of

$$\mathbf{w}^T(\theta_k) = \begin{bmatrix}-r(\theta_k) & 1\end{bmatrix}, \tag{58}$$

where $r(\theta_k)$ is the monopulse ratio for angle, θ_k. Applying equation (58) results in

$$x(k) = \Delta(k) - r(\theta_k)\Sigma(k). \tag{59}$$

Recognizing that ideally $\Delta(\theta_k)/\Sigma(\theta_k) = r(\theta_k)$, it is obvious that this nulls the energy from the direction, θ_k. We emphasize that we can choose the null direction, θ_k, on a pixel-by pixel basis. Typically, we choose the angles, θ_k, to be in the estimated direction of unwanted clutter so as to eliminate clutter.

An issue with the previous technique is that the sole purpose is to eliminate return from direction θ_k without regards to the attenuation of the desired signal in the direction, θ_t. This suggests the second method that we consider, which is to develop the weight vector to minimize the return subject to the constraint as follows†

$$\mathbf{w}^H(k)\bar{\mathbf{c}} = 1, \quad \text{with}$$
$$\bar{\mathbf{c}}^T = \begin{bmatrix} 1 & r(\theta_t) \end{bmatrix}. \tag{60}$$

The result of enforcing this constraint is that after applying the filter the return from the desired angle, θ_t, will be just the return expected from $\Sigma(\theta_t)$, while other targets will be minimized in an optimal way. Basically, we wish to retain gain in the desired direction and do the best we can at nulling in the interfering direction.

We illustrate the difference between the two filter choices with the following example. Consider a 6º beamwidth, a normalized monopulse ratio $k_m = 1.5$, "Clutter" to Noise Ratio (CNR) of 20 dB, and a desired target location at the null, i.e., at $\theta_t = 0^{\circ}$. Figure 10 shows the signal attenuation‡ as a function of angle, θ_k, due to nulling. Figure 11 shows the attenuation of the undesired "clutter" return at angle θ_k given the desired return at the angle $\theta_t = 0^{\circ}$.

We see that the first, non-constrained, method attempts to null the undesired signal at the expense of partial attenuation of the desired signal. This loss in the desired signal response increases as the undesired return angle approaches the desired return angle location. The second, constrained, method maintains unit gain in the direction of the desired return, $\theta_t = 0^{\circ}$, but has a limitation on the attenuation of the undesired return at angle, θ_k. The normalized monopulse ratio slope, k_m, plays an important role in the limits of both of these methods.

Note that the above results make sense for an amplitude monopulse, but for a phase monopulse we need to multiply one of the vector components in equation (58) by the appropriately signed value of the imaginary number, j.

---

† This is essentially the monopulse equivalent of the Minimum Variance Distortionless Response (MVDR) filter.

‡ This is actually a gain that is negative. More negative values represent more loss.

The result of the above is that we can generate a null on a pixel by pixel basis provided that the estimated angle information, $\hat{\theta}_k$, is correct.

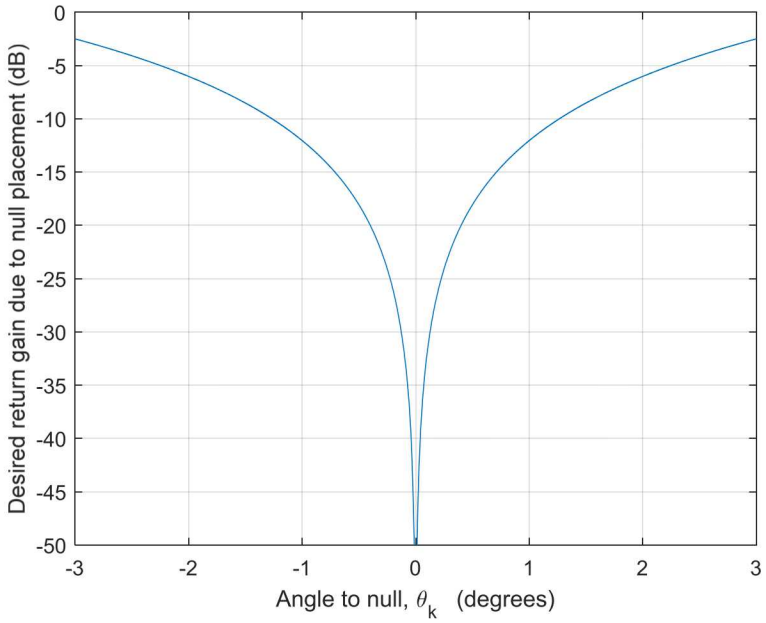

Figure 10. Example signal loss (really gain) at $\theta_t = 0^o$ for a given clutter/interference angle, θ_k .

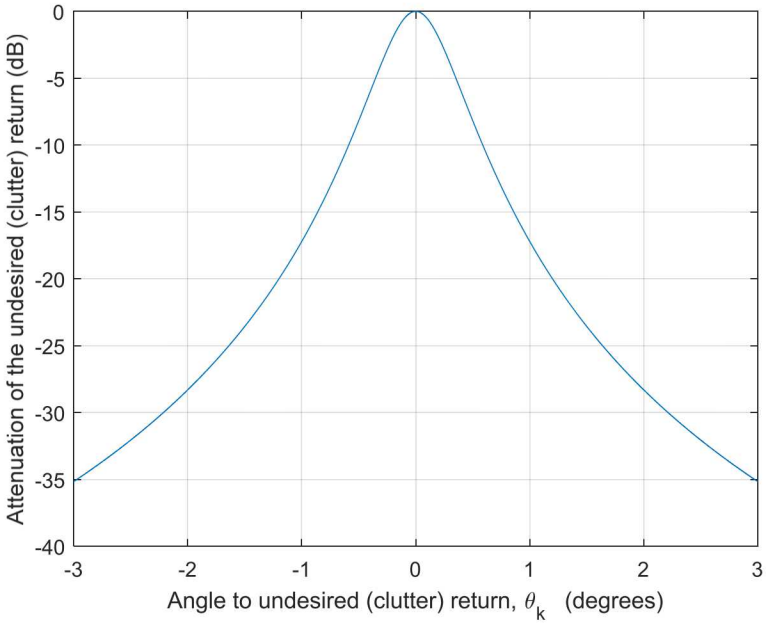

Figure 11. Example clutter/interference loss (really gain) at angle, θ_k for the desired return at $\theta_t = 0^o$.

“We don't know a millionth of one percent about anything.”
-- Thomas A. Edison

5 Conclusions

We repeat some key points.

- The direction of a monopulse null can be steered for both phase-monopulse systems and amplitude-monopulse systems, even for a single radar pulse.

- Phase-monopulse systems are steered by adjusting phase-shifts to the individual subapertures' phase-centers.

- Amplitude-monopulse systems are steered by adjusting relative gains to the individual lobes. This may be accomplished by adding sum-channel signal to the difference channel.

- As the null is steered to a different DOA, the monopulse slope in the vicinity of the null will change somewhat, but generally not a great deal.

- By adjusting the null steering to compensate for a rotating antenna, the null DOA may be stabilized, although the monopulse slope will exhibit some slight modulation.

“Always do whatever's next.”
-- George Carlin

References

[1] *IEEE Standard Definitions of Terms for Antennas*, IEEE Standard 145-1983, The Institute of Electrical and Electronics Engineers (IEEE), 22 June 1983.

[2] Samuel M. Sherman, David K. Barton, *Monopulse Principles and Techniques – second edition*, ISBN-13: 978-1-60807-174-6, Artech House, Inc., 2011.

[3] Douglas L. Bickel, *Precomparator and Postcomparator Errors in Monopulse*, Sandia National Laboratories Report SAND2013-1287, Unlimited Release, February 2013.

[4] F. M. Staudaher, Chapter 16: "Airborne MTI", in *Radar Handbook*, M. I. Skolnik, ed., 2nd edition, McGraw-Hill, 1990.

[5] Armin W. Doerry, Douglas L. Bickel, *GMTI Direction of Arrival Measurements from Multiple Phase Centers*, Sandia National Laboratories Report SAND2015-2310, Unlimited Release, March 2015.

[6] Armin W. Doerry, Douglas L. Bickel, *Limits to Clutter Cancellation in Multi-Aperture GMTI Data*, Sandia National Laboratories Report SAND2015-2311, Unlimited Release, March 2015.

[7] Armin W. Doerry, Douglas L. Bickel, *Phase Centers of Subapertures in a Tapered Aperture Array*, Sandia National Laboratories Report SAND2015-9566, Unlimited Release, October 2015.

[8] Armin W. Doerry, Douglas L. Bickel, *Single-Axis Three-Beam Amplitude Monopulse Antenna – Signal Processing Issues*, Sandia National Laboratories Report SAND2015-4113, Unlimited Release, May 2015.

[9] Armin W. Doerry, *Just Where Exactly is the Radar? (a.k.a. The Radar Antenna Phase Center)*, Sandia National Laboratories Report SAND2013-10635, Unlimited Release, December 2013.

Distribution

Unlimited Release

Hardcopy Internal

1	A. W. Doerry	5349	MS 0519
1	L. Klein	5349	MS 0519
1	M. R. Lewis	5349	MS 0519
1	S. P. Castillo	5340	MS 0532

Email—External

Brandeis Marquette	Brandeis.Marquette@ga-asi.com	General Atomics ASI
Jean Valentine	Jean.Valentine@ga-asi.com	General Atomics ASI
John Fanelle	John.Fanelle@ga-asi.com	General Atomics ASI

Email—Internal

Technical Library	9536	libref@sandia.gov

Sandia National Laboratories is a multimission laboratory managed and operated by National Technology & Engineering Solutions of Sandia LLC, a wholly owned subsidiary of Honeywell International Inc. for the U.S. Department of Energy's National Nuclear Security Administration under contract DE-NA0003525.